Research Square

Preprints are preliminary reports that have not undergone peer review.
They should not be considered conclusive, used to inform clinical practice,
or referenced by the media as validated information.

Pulse Physiology Engine to simulate transient oxygen changes and closed-loop, autonomous pump control during venovenous extracorporeal membrane oxygenation

Rei Ukita

rei.ukita@vumc.org

Vanderbilt University Medical Center https://orcid.org/0000-0002-3523-6182

Sriya Bapatla

Vanderbilt University

Jeffrey Webb

Kitware (United States)

Aaron Bray

Kitware (United States)

Yerin Woo

Vanderbilt University Medical Center

Andrew R Kumpfbeck

Vanderbilt University Medical Center

Steven P Keller

Johns Hopkins University

Rachel B Clipp

Kitware (United States)

Research Article

Keywords: computer simulation, extracorporeal membrane oxygenation, automation, proportional-integral derivative (PID) controller, time constant, digital twin

Posted Date: November 3rd, 2026

DOI: https://doi.org/10.21203/rs.3.rs-11569452/v1

License: This work is licensed under a Creative Commons Attribution 4.0 International License.
Read Full License

Additional Declarations: The authors declare potential competing interests as follows: R.U. is a co-inventor on a patent application US20250205468A1 “Smart programmable blood pump for controlling and automating extracorporeal life support applications.” J.B.W., A.B., and R.C. are employees at Kitware, Inc.

Abstract

Venovenous extracorporeal membrane oxygenation (VV-ECMO) is a lifesaving respiratory support therapy growing in clinical volume worldwide. Its physiology is complex, yet management strategies vary widely across centers. Meanwhile, patient-to-patient variability makes standardization difficult. To address these challenges, we previously presented a patient-specific model of VV-ECMO based on the Pulse Physiology Engine (Pulse). However, previous study's scope was limited to validating steady-state physiology. This work (1) compares transient venous oxygen saturation (SvO_2) simulations in Pulse to *in vivo* pig data, (2) implements pump speed as a model input, and (3) simulates closed-loop pump control using proportional integral (PI) controller. The time constants from SvO_2 simulations show significant, positive correlations with *in vivo* data (coefficient=0.929, $p<0.001$). Furthermore, both experimental and simulated time constants show significant, negative correlation with their corresponding blood flow ($p<0.05$). With pump speed as model input, the model predicts achieved blood flow rate in two different clinical systems with reasonable accuracy. Finally, a well-tuned PI pump controller can reject disturbances induced by the ventilator, while there should be precautions for setpoint SvO_2 change and oxygenator thrombosis. Future work will validate the closed-loop findings in a large animal model to bring Pulse closer towards a digital-twin model of VV-ECMO patients.

Clinical Trial Registration

not applicable

1. Introduction

Extracorporeal membrane oxygenation (ECMO) is increasingly used as an advanced life support therapy for end-stage lung diseases and failures. ECMO circuits use pumps, cannulas, and membrane oxygenators to drain deoxygenated blood from the patient and to return oxygenated blood to the patient. Over the last 5–10 years alone, more ECMO cases have been reported to the international registry than in the preceding 30 years, reflecting the explosive growth in the number of centers and the volume of cases.[1] Despite this growth, ECMO still has room for improvement in both efficiency and efficacy. Optimal management and titration of ECMO parameters (e.g., blood flow and sweep) currently rely on manual, experience-based adjustments rather than a standardized protocol across centers.[2–4] Meanwhile, developing a universal protocol for all patients is also difficult, given the wide variability in anatomy, clinical status, and lung disease severity across individuals.

A computer simulation platform for ECMO physiology offers one path toward standardizing care across centers.[5–8] Such a model can recommend a precise level of ECMO support needed to elicit a target physiological response (e.g., arterial oxygen content and pH). By tailoring input parameters, the model can also account for patient- and case-specific differences. Our team previously presented a computational model of VV ECMO physiology, built on the Pulse Physiology Engine (Kitware Inc.) that takes patient-specific parameters (weight, sex, lung disease severity) and device-specific parameters

(mechanical ventilation and ECMO circuit settings) as inputs and simulates the patient's physiological response.[8] The previous Pulse ECMO model showed appropriate simulated responses to changes in ECMO flow, sweep, and FdO_2, where the changes were comparable in magnitude to those reported in a 2013 study by Schmidt et al.[9] This prior simulation study also demonstrated the model's capacity to simulate transient responses to ECMO blood pump changes over time; however, the accuracy of transient physiological oxygenation modeling has not been quantified.

This study addresses that gap by evaluating the model's fidelity in simulating patients' transient physiological responses to blood flow changes by comparing the simulated results to data collected from a large animal porcine model of lung dysfunction and VV-ECMO. The study will then use this transient modeling capability of Pulse Physiology Engine to enable *in silico* investigations of closed-loop automated control of ECMO to generate insights about automated blood pump control strategies.

2 Methods

2.1. Pulse Overview

This work uses the Pulse Physiology Engine (Pulse for short), an open-source whole-body computational physiology platform that has demonstrated versatility across a range of medical simulation, device integration, and research applications that now includes VV ECMO (Fig. 1A, **Table S1**).[8,10] Each physiological system in Pulse is represented as a zero-dimensional, lumped-parameter circuit analog with integrated homeostatic feedback. The differential equations governing all systems are solved simultaneously through transient analysis at a shared dynamic timestep of 20 milliseconds, maintaining real-time execution while preserving numerical stability. Medical device models, including mechanical ventilators[11] and extracorporeal circuitry[8] are implemented within the same mechanistic framework as the patient physiology, preserving the fidelity of device-patient interactions throughout the simulation. Pharmacokinetic and pharmacodynamic behaviors can also be integrated to study drug effects.

Cardiovascular and respiratory systems in Pulse are tightly coupled at the alveolar-capillary interface, where gas exchange is governed by partial pressure gradients of oxygen and carbon dioxide and is modulated by ventilation-perfusion matching. This integration allows Pulse to dynamically adjust cardiac output, respiratory rate, and tidal volume in response to evolving blood gas levels, thereby reproducing the compensatory responses central to VV-ECMO physiology. The circuit solver centralizes the lumped-parameter network mathematics across all systems and handles nonlinear components, dynamically changing topologies, and time-varying parameters while the substance transporter enforces conservation of mass and energy to update compartment-level gas concentrations and volumes at each timestep.

The Pulse software architecture is built around a common data model that standardizes patient definitions, physiological conditions, clinical actions, substances, and equipment configurations. Since the previous study, the VV-ECMO circuit model and associated physiology extensions have been

implemented in the core C + + engine.[8] In this study, Python bindings were used to configure scenarios and perform validation analyses. This separation allowed model development to remain tightly coupled to the numerical solvers while enabling rapid testing and reproducibility at the scenario level.

2.2. Pig VV-ECMO Study

All animal procedures were reviewed and approved by the Institute for Animal Care and Use Committee at Vanderbilt University Medical Center and by the Animal Care and Use Review Office at the United States Army Medical Research and Development Command. All large animal experiments were performed in accordance with institutional and federal guidelines and regulations, including the ARRIVE 2.0 (Animal Research: Reporting In Vivo Experiments) guideline.

Yorkshire x Landrace pig (N = 5, 61–87 kg) was procured from Oak Hill Genetics (Ewing, Illinois). Pigs were induced with an intramuscular dose of xylazine (2.2 mg/kg), tiletamine and zolazepam (4.4 mg/kg), and ketamine (2.2 mg/kg). An endotracheal tube was placed for airway access, and during extracorporeal support, the lungs were ventilated at a tidal volume of approximately 4 mL/kg. The ventilator FiO_2 was set to 21%, the respiratory rate to 18 breaths per minute, and the PEEP to 5 cm H_2O. Total intravenous anesthesia was maintained with propofol (maximum rate: 3.5 mg/kg/hr), midazolam (maximum rate: 0.5 mg/kg/hr), and fentanyl (maximum rate: 10mcg/kg/hr). The pig was placed on VV-ECMO under bilateral femoral cannulation with either a single-site, dual-lumen strategy (N = 2 for 28-French, N = 2 for 20-French dual-lumen cannula), or dual-site, single-lumen strategy using a 19- French drainage and a 21- French reinfusion cannulas (N = 1). The extracorporeal circuit used a Spectrum Medical Quantum CP22 centrifugal blood pump and a Medtronic Nautilus oxygenator for all studies. The centrifugal pump was driven by a Smart Blood Pump system described previously.[12] Terumo CDI Blood Parameter Monitoring System 550 and a 3/8" x 3/8" H/S cuvette sensor were used to obtain real-time venous hemoglobin and saturation levels at the oxygenator blood inlet. A Transonic flow meter (TS410) and probe (ME9PXL) were used for blood flow rate measurements. The blood flow rate was step increased or decreased which yielded a slower response as change in venous oxygen saturation. Sweep gas flow was constant during blood flow step changes. Each blood flow step was maintained until inlet venous oxyhemoglobin (SvO_2) reached steady state (Fig. 2A). Real-time trajectories of blood flow and SvO_2 were collected using ADInstruments PowerLab and LabChart and processed in MATLAB R2025a. At the end of the animal study, the pig was euthanized with an intravenous dose (> 120 mg/kg) of pentobarbital sodium.

For data analysis, curve fitting was performed in MATLAB to approximate SvO_2 trajectories as an exponential function of time in seconds: $SvO_2(t) = a_1 - a_2 \exp(-t/\tau)$, where τ is the time constant. The time constants values from these animal studies were used to compare to the time constants derived from Pulse simulations. The Pulse simulation counterparts were run using the same settings as the animal experiment in terms of body weight, extracorporeal blood flow, and sweep. The following ventilator settings were used for comparing to the pig experimental data: tidal volume of 4 mL/kg body weight, inspiratory flow of 60 L/min, ventilatory period of 0.9 seconds, fraction of inspired oxygen of 21%,

positive end expiratory pressure of 5 cm H_2O, and respiratory rate of 18 breaths per minute. To ensure that the pig experiment and the simulation had comparable initial venous oxygen conditions, a pulmonary shunt was incrementally adjusted in the simulation until the ECMO inlet venous oxygen saturation was within 2 percentage points of the experimental value measured at the start of step changes. For the pig VV-ECMO experiment time constant data and the simulated counterparts, pooled results are presented as mean ± standard deviation. Repeated-measures correlation, originally presented by Bakdash and Marusich,[13] was performed to analyze blood flow rate after the step change and the corresponding SvO_2 time constant generated from the experimentt and the simulation. To run this statistical analysis, a web application developed by the same authors was used,[13,14] and a p-value less than 0.05 was deemed significant.

2.3. Pulse Modeling Approach

The model parameters were similar to as described in the previous publication.[8] The default extracorporeal circuit settings are summarized in **Table S2**.

2.3.1. Pressure-Flow Characteristics: To enable pump speed as an input to the Pulse Physiology Engine framework (Fig. 1B), a custom script was written in Python to relate pressure-flow characteristics between extracorporeal circuit components (pump, oxygenator, cannula, and tubing) following the methods presented previously.[15,16] This approach applies Kirchoff's voltage law equivalent to the venovenous extracorporeal circuit to solve for flow based on known circuit resistance profile, pump performance curves, and pump speed. Using published data, empirical polynomial relationships were developed to relate centrifugal pump speed (RPM), pressure head (P), and flow rate (Q): $P(Q, RPM) = a_1Q + a_2 Q^2 + a_3 RPM^2$. The Maquet Rotaflow polynomial equation was approximated using a 2006 study by Ganushchak and colleagues,[17] and the Sorin Revolution's was taken from a 2025 study by Glomp and colleagues.[18] Instead of treating cannula resistance as a fixed value as done in the previous work,[8] cannula resistance was modeled here as a quadratic function: $P = a_1Q + a_2Q^2$, using relevant publications. Specifically, Maquet Avalon dual-lumen cannula resistance profile was taken from a 2019 study by Wang and colleagues that evaluated pressure-flow characteristics using a 27% hematocrit fluid.[19] The cannula resistance values were continually updated during the simulation based on changes in circuit pressure and/or flow. Maquet Quadrox resistance was assumed as a fixed resistance of 5.5 mmHg/L/min based on a 2026 study by Sabetta and colleagues.[20] ECC05 oxygenator resistance was approximated as 30 mmHg/L/min based on the 2014 study by Lehle et al.[21] Tubing resistance and pressure drop was set to 1.5 mmHg/L/min for both drainage and reinfusion limbs, assuming 100 cm length for each. These device specifications were used in all sections of Pulse modeling described herein.

To validate this pump speed input modeling framework, simulations were performed using a prior clinical study by Lehle et al, which showed the relationship between pump speed and corresponding blood flow achieved for VV-ECMO patients supported by four different device configurations.[21] Out of

those four combinations studied, Maquet Rotaflow-Quadrox and Sorin Revolution–ECC 05 were chosen to compare to the calculated blood flow rate since those two were the only device combinations that have published data on pump and oxygenator performances, as noted in the previous paragraph. Both of these combinations used 27-French Avalon dual-lumen cannula. Lehle et al's study presented their pump speed-flow relationship as individual data points overlaid with a line of best fit over those points. The linear fits were therefore used to compare the simulations run in Pulse Physiology Engine with the same devices.

2.3.2. Closed-Loop Control of Blood Pump: After the RPM input feature was implemented, the entire simulation framework was used to model VV-ECMO under a closed-loop, automated control scheme. The base patient condition was a standard 70-kg male model on Pulse experiencing an acute pulmonary shunting at a severity of 0.70 on mechanical ventilation under volume control with the following settings: tidal volume of 200 mL, inspiratory ventilator flow of 60 L/min, ventilatory period of 0.9 seconds, fraction of inspired oxygen of 75%, positive end expiratory pressure of 5 cm H_2O, and respiratory rate of 18 breaths per minute. Thereafter, ECMO was initiated under VV configuration using Quadrox, Rotaflow, and Avalon dual-lumen cannula with diameter of 20, 27, or 31 French. The initial blood flow was set to about 1 L/min and the corresponding pump speed for the first 150 seconds of simulation prior to starting the automatic control. The fraction of oxygen in the sweep (FdO_2) was fixed at 100%, and sweep was also fixed at 5 L/min for the entire simulation including the automated phase. For Quadrox, the initial value for oxygenator's oxygen diffusion capacity was set to 0.53 mL O_2/min/mmHg based in the manufacturer's data as done previously.[8] Blood pump automation was implemented as a proportional integral (PI) controller using venous blood oxyhemoglobin saturation (SvO_2) as a target parameter and its setpoint between 60 and 80% (Fig. 1C). The initial estimates for the PI gain coefficients, Kp and Ti, were determined using a MATLAB PID tuner using the porcine blood flow step testing data described earlier. Based on the results, different sets of Kp and Ti were chosen to parametrically evaluate controller performance in terms of stability and rapidity: Kp = [1000, 4000], and Ti = [10, 36] seconds. As automatic controller safety measures, the Rotaflow pump speed was set to maximum speed limit of 4000 RPM and minimum of 500 RPM, and maximum rate of increase or decrease at 200 RPM/second. Anti-windup was also implemented into the PI control structure when pump speed reached an upper or lower limit to prevent accumulation of error term due to saturation.

Disturbance Rejection Testing: One of the following disturbances was introduced at 1200 second mark after starting the automated control with Kp = 4000 and Ti = 36 s: step change in the setpoint SvO_2, change in ventilator setting, or acute thrombotic failure of oxygenator. Setpoint increase and decrease by 10 percentage points from the default setpoint of 70% were both tested. Ventilator setting change was modeled as FiO_2 step-decreased from 100% to 75, 50, or 21% coupled with tidal volume decreased from 200 mL to 150, 100 or 50 mL. Acute oxygenator thrombosis was modeled as an increase in resistance to 11, 30, and 55 mmHg/L/min coupled with decrease in oxygen diffusion capacity to 0.30, 0.20, or 0.10 mL O_2/min/mmHg.

Controller Performance Analysis

Standard quantification of controller stability consisted of computing flow rise time, flow overshoot, and time to steady-state SvO_2. The blood flow rise time was calculated as the time to get from 10% to 90% of the steady state flow. The flow overshoot percentage was computed as ($Q_{max} - Q_{ss})/(Q_{ss} - Q_{initial}) \times 100\%$ where Q is blood flow and the subscripts *max*, *ss*, and *initial* represent maximum, steady-state and initial, respectively. The time to steady-state SvO_2 was calculated as the amount of time required for SvO_2 to settle within 1 percentage point of the setpoint.

3. Results

3.1. Pig VV-ECMO Study

The exponential time constants obtained from the SvO_2 trajectories (Fig. 2A) during porcine VV-ECMO experiments were 87 ± 48 seconds (N = 12 across 5 animal subjects). The corresponding blood flow rate after the step change was 2.21 ± 1.14 L/min. There was a significant, negative correlation between time constant and flow rate from these experiments (Fig. 2B, correlation coefficient = − 0.73, p = 0.041). The time constants obtained from simulated VV-ECMO using the same flow step changes were 112 ± 34 seconds. Like the porcine experimental findings, there was a significant, negative correlation between the simulated time constants and the corresponding flow rate (Fig. 2C, D, coefficient = − 0.713, p = 0.047). Furthermore, the time constants obtained from the simulations and the experiments exhibited significant, positive correlation (Fig. 2E, coefficient = + 0.929, p < 0.001)

3.2. Pump Speed as Model Input

The pump speed input feature was validated using a 2014 study by Lehle and colleagues which characterized flow-pump speed relationship. Figure 3A shows simulation results showing the Maquet Rotaflow pump curves at varying speeds superimposed with the system curve that represents resistance contributions from the Maquet Quadrox and the Maquet Avalon 27-French dual-lumen cannula. Their intersection denotes the pressure and flow achieved for the specific input speed. Figure 3B shows the simulated Maquet Rotaflow flow values in comparison to the linear fit presented in the original Lehle publication for varying input pump speeds. At Rotaflow pump speeds of 1000, 2000, 3000, and 4000 RPM, the Pulse model predicted flow rates of 0.87, 2.08, 3.31, and 4.56 L/min. In comparison, the estimated flow values at the same speeds from the original publication's values from the linear fit were 0.97, 1.94, 2.91, and 3.88 L/min. Figures 3C and **D** similarly show the data for Sorin Revolution pump and ECC05 oxygenator. At Sorin pump speeds of 1000, 2000, and 3000 RPM, the simulated flow values were 0.72, 1.99, and 3.36 L/min, in comparison to the original publication values of 1.3, 2.6, and 3.9 L/min. Rotaflow simulations underestimated at low speeds and overestimated at high speeds, such that error magnitude at each speed between 1000 RPM and 4000 RPM were + 10.5, − 7.1, − 13.9, and − 17.4%, respectively. Meanwhile, Sorin simulations underestimated the flow for all speeds and displayed greater

errors than Rotaflow in magnitude but decreased with increasing pump speed. Errors at 1000, 2000, and 3000 RPM were, respectively, + 44.8, + 23.5, and + 13.8%.

3.3. Closed-Loop ECMO Pump Control

Closed-loop control of ECMO blood pump using speed as an input parameter was demonstrated under different scenarios. First, the controller performance and physiological response are presented for a fixed set of patient and circuit configurations while varying the controller gain coefficients and dual lumen cannula sizes (Fig. 4). Under a default setting of 27 French Avalon (Fig. 4, middle column), there were notable differences in the rapidity and stability across gain settings. Flow rise time was the fastest in the high Kp = 4000 and low Ti = 10 s condition at 8 seconds, but it also exhibited the largest overshoot at 144.5%. On the other hand, Kp = 1000 and Ti = 36 s had the slowest rise time of 698 seconds, lowest overshoot of 0.65%, and the longest time to steady state of 781 seconds. The two intermediate conditions (Kp = 1000 and Ti = 10s, Kp = 4000 and Ti = 36) fell between the two extremes, such that the rise time was between 46 and 82 seconds, overshoot between 20 and 27%, and time to steady state between 178 and 195 seconds. For sensitivity analysis, the dual-lumen cannula size was changed to either 20 French or 31 French and then reevaluated for controller performance with the same set of gain coefficients. Compared to the 27-French, the 31-French cannula scenario exhibited faster responses such that the rise time was between 12 and 51 seconds for the two intermediate gain settings, but had higher overshoots between 37 and 48% (Fig. 4, right column). In the 20-French scenario, three of the four gain settings resulted in pump speed reaching an upper threshold of 4000 RPM, whereas the remaining fourth gain setting did not reach a steady state after the full simulated duration of 1200 seconds (Fig. 4, left column). **Table S2** provides the full controller analysis for these scenarios. For all subsequent controller simulation data, the circuit configuration will be a VV-ECMO circuit consisting of 27-French Avalon, Quadrox, and Rotaflow, and pump controller gain coefficients of Kp = 4000 and Ti=36s.

3.3.1. Disturbance Scenarios

The controller was assessed for disturbance rejection under three different scenarios – ventilator change (Fig. 5), SvO_2 setpoint change (Fig. 6), and acute thrombosis (Fig. 7). In the ventilator-induced disturbance scenario, the steady-state values for pump speed and flow increased with the magnitude of reduction in vent FiO_2 and tidal volume (Fig. 5B, C). The overall magnitude of change in SvO_2 and SaO_2 was less than 2 percentage points for all scenarios (Fig. 5D, E). Acute setpoint changes led to varying performances depending on the magnitude and the direction of change. Increasing setpoint to 87.5% caused the pump to reach maximum speed, whereas there was undershooting behavior when the setpoint was decreased to 62.5%. The two intermediate setpoint changes (67.5 and 82.5%) did not demonstrate either of these behaviors. Acute oxygenator thrombosis, modeled as a step increase in resistance and a step decrease in membrane O_2 diffusion capacity at 3 distinct levels, caused acute drops in oxygenator outlet P_{O2} and blood flow that were proportionate to the level of change in those oxygenator coefficients. This was followed by a slower decrease in SvO_2 over time that was partially or

fully addressed the pump controller's speed and flow increase. For the most severe thrombotic case (resistance = 55 mmHg/L/min, diffusion capacity = 0.10 mL/min/mmHg), the pump reached its maximum speed while the steady-state SvO_2 stabilized at 67%, 8 percentage points below the setpoint.

4. Discussion

Here we report on the expanded simulation platform for VV-ECMO based on the Pulse Physiology Engine. The model was used to simulate transient oxygenation physiology and compared to porcine VV-ECMO experimental data. Then, the pump speed input was implemented to allow control over specific pump models tied to their pressure-flow characteristics. The inputted pump speeds and the corresponding blood flow rates were compared to previously published data for accuracy.[21] Finally, this new transient modeling framework was used to simulate a closed-loop control of blood pump under different physiological disturbance scenarios

The porcine experimental data showed that the change in venous oxygen level is a slow process on the order of minutes for moderate flow rate below 4 L/min (Fig. 2B), and the simulated time constants were also within this range (Fig. 2D). While the absolute time constants values were different between simulated and experimental findings, there was a strong positive corrleation between the two (Fig. 2E, coefficient = 0.929). Furthermore, the time constant's negative correlation with blood flow rate were noted in both simulations and experiments. The statistical findings are not surprising, as faster extracorporeal blood flow rate should shorten the time for oxygenated blood to reenter the patient's systemic circulation and lead to steady state more quickly. The markedly low time constant in the porcine experiment at 5 L/min compared to the simulated results may be explained by this venous recirculation. Recirculation is known to increase with extracorporeal blood flow rate,[22,23] yet this phenomenon was not explicitly modeled in Pulse. It is possible to combine the zero-dimensional Pulse model with a three-dimensional fluid dynamics model based on patient anatomy and cannula positioning.[24,25] Hence, a more advanced modeling approach may yield higher physiological accuracy by accounting for geometric influences. Nevertheless, Pulse was able to recreate this physiological trend between process time characteristics of oxygenation and extracorporeal blood flow, which has important implications for pump controller design.

The presented modeling framework was modified to use pump rotational speed as an input variable to better reflect clinical applications (Fig. 3). Since the base Pulse ECMO model only takes blood flow rate as input, an additional computational step was used to first calculate the flow rate based on pump speed and circuit characteristics. This approach follows previously described lumped parameter models that use empirical pressure-flow relationships of ECMO components.[15,16] To validate this pump speed input feature, data from a prior study by Lehle and colleagues were used, given the wide range of pump speeds and flow rates that their work reported across multiple device models.[21] Meanwhile, only two out of the four device combinations – Maquet and Sorin – were chosen since they were the only sets of pump-oxygenators with well-characterized pressure-flow relationships in the literature.[17,18,20,21] In the

Maquet combination with Quadrox and Rotaflow, the simulations error magnitudes were below 20%, and they overestimated flow at higher RPM and underestimated at lower RPMs. This agrees with the author's prior study, which used lumped parameter model to predict ECMO blood flow.[15] Like that previous work, there are likely minor losses that are not captured by the lumped parameter model which can come from tubing, connectors, cannulas, and devices. Meanwhile, the Sorin simulation consistently underestimated flow rate by as much as 45%. One potential source of error is the limited availability of Sorin data on their pressure-flow characteristics compared to those of Maquet. The Maquet Rotaflow and Quadrox pressure-flow characteristics have been repeatedly studied by multiple research groups with good reproducibility,[26,27] whereas the authors could only find one published study on Sorin Revolution's pressure-flow curves, which is also the author's own work.[18] Similarly, there were no reliable data for ECC05 oxygenator resistance other than what was provided in the Lehle et al's study.[21] Hence, the Sorin simulation results may be biased by this limited data availability. Nevertheless, this level of accuracy should be adequate for reasonably estimating achievable flow rate for a given pump speed and VV circuit characteristics. This feature can help diagnose problems with the circuit such as thrombosis or cannula malposition, which would cause a mismatch between observed and theoretical flow rates of a circuit.

With the new speed input feature, Pulse-based platform can be reliably used to simulate closed-loop control of blood pumps and to optimize its performance. Rapidity and stability are both important design variables to consider, since the pump should respond to acute oxygen level changes without changing its pump speed too quickly, which has hemolysis risks.[28] The presented simulation platform can help support this co-optimization process. To illustrate this capability, we first showed a PI controller under varying gain settings to maintain a setpoint venous oxygen level (Fig. 1C). Here, SvO_2 was selected as a setpoint parameter since it can be directly linked to oxygenation, and also because it can be measured in real time using oximetry probe at the oxygenator inlet as demonstrated (Fig. 2A).[29,30] Proportional integral controller is also a simple yet robust strategy for automation but requires tuning *a priori* to achieve desirable performance. Running simulations with various combinations of gain coefficients, as shown here, could achieve some level of tuning before actual implementation of ECMO controller. The most favorable performance for 27-Fr and 31-Fr cannulas was achieved with either Kp = 4000 and Ti = 36 or Kp = 1000 and Ti = 10 (Fig. 4). In those two larger cannula sizes, flow and SvO_2 signals were underdamped and oscillatory at the gain settings of Kp = 4000 and Ti = 10, whereas they were overdamped and slow for Kp = 1000 and Ti = 36. Meanwhile, the 20-Fr cannula scenario showed overdamped performance across all gains due to reaching maximum speed of 4000 RPM, a limit selected based on maximum RPM reported by the Lehle et al study.[21] The simulations here demonstrate the importance of optimizing controller gain settings based on the specific circuit characteristics to limit underdamped behaviors that can increase hemolytic risks, as well as overdamped behaviors that can limit oxygen adequacy.

We also show that the PI control strategy's ability to reject physiological disturbances and maintain oxygen homeostasis. We evaluated four different scenarios: (1) reduction in ventilator FiO_2 and tidal

volume (Fig. 5), (2) change in the control setpoint SvO_2 (Fig. 6), and (3) acute thrombotic occlusion of oxygenator (Fig. 7). The simulations here showed that a tuned PI controller can sense and correct blood oxygen disturbance caused by a change in native lung perfusion-ventilation profile, most notably in the scenario with acute change in the ventilator setting. While the ventilatory setting change is abrupt, the overall effect on the blood oxygen level is a slow process that is rate-limited such that the pump controller can respond and address with ease. Both the magnitude and the rate of change in SvO_2 generally match values reported by Conway and colleagues, whose study used a sudden ventilator shut-off as a disturbance scenario in sheep to evaluate their automated pump controller.[31] After their vent shut-off, SvO_2 dropped gradually from about 73% to 68% over 90 seconds before it recovered from the automated pump control.[31] Meanwhile, the simulated scenarios herein were more moderate – a step decrease of FiO_2 and tidal volume – as opposed to the complete shutoff by Conway et al. The findings here suggest that a pump controller is able to promptly address respiratory disturbances due to the slow overall process characteristics of oxygenation.

The SvO_2 setpoint disturbance scenario shows a potential limitation of a linear PI pump control strategy. While the controller responded to an increased setpoint without any overshoots, the pump speed reached the maximum limit of 4000 RPM when the setpoint was set high at 87.5%. A few precautions should be put in place. First, anti-windup scheme needs to be programmed into the PI controller to ensure that there are no additional accumulations of error terms when maximum or minimum limits are reached. Second, the setpoint SvO_2 should not be set too high to avoid these situations in the first place. Meanwhile, the controller exhibited an undershooting behavior when the setpoint was decreased from 75 to 62.5%. This can be largely ascribed to the circuit's nonlinear resistance profile, which was shown earlier as system curves in Fig. 3A and **C**. The cannula pressure drop scales quadratically with flow, so a fixed pump speed increment will yield smaller corresponding increase in flow as the speed gets higher. In comparison, a fixed pump speed decrement will yield a relatively larger decrease in flow, resulting in undershoot as seen here. There may be several ways to address this. For instance, there can be an asymmetric, gain scheduling strategy so that the controller separately addresses flow increase versus decrease. Additionally, there should be a limit on the relative change in setpoint from the current value so that it does not produce a large error in a short amount of time.

Thrombotic occlusion of oxygenators could be addressed by the PI control strategy to some extent. This was simulated with a combination of increase in the oxygenator resistance and decrease in the oxygen membrane diffusion capacity. The immediate result is a drop in extracorporeal blood flow and a drop in the oxygenator's blood outlet oxygen content (Fig. 3B, D), followed by a gradual decrease in the venous saturation (Fig. 3E). The PI controller responds to dropping saturation by increasing pump and speed blood flow rate to compensate (Fig. 3C, D), but the controller may reach its maximum limit depending on the severity of failure. The oxygenator failure simulation here is exaggerated as a step change in resistance and oxygen diffusion capacity, but this is not too far off from how it manifests clinically. In reality, oxygenator resistance can exponentially increase due to rapid thrombotic occlusion.[32] Likewise, oxygenator outlet oxygen content can also drop due to clot formation obstructing gas exchange fiber

surfaces.[32] Increasing pump speed to maintain flow through circuit with a large clot burden would increase local shear and accordingly hemolytic risks, so this would be an instance where automated control can worsen clinical status. Automated controller should therefore be further informed by pressure monitoring to ensure that the pump speed can be safely increased.

There are several limitations to this study that need to be acknowledged. First, the Pulse model is designed for human physiological simulations, whereas the experimental data were taken from pig studies. The simulations were run to reflect the experiment in terms of animal size, circuit configuration, and ventilatory settings. Regardless, there can be innate species-dependent factors that cannot be closely modeled. Future work will use human clinical data to validate transient physiology. Additionally, this study did not evaluate transient physiology of CO_2 removal, which will be pursued in future works. There are also several limitations pertaining to the implementation of closed-loop pump control. Simulations here were all done with the same baseline case of a standard male patient with a pulmonary shunt pathophysiology. We also only focused on PI control strategy using SvO_2 as a setpoint. Simulating different patient demographics, lung diseases, or control strategies could offer other insights that may conflict what were shown here. Furthermore, the simulations of automated blood pump control have not been validated yet with real-life data. Since a closed-loop ECMO blood pump controller does not exist clinically, future work will need to validate the findings here with animal studies.

5. Conclusion

In summary, we presented on Pulse Physiology Engine as a viable platform for simulating transient physiology of extracorporeal blood oxygenation that now includes the capability to model blood pump speed control. We highlight the utility of this model by demonstrating various use cases for closed-loop automated control of the pump. One of the strengths of this simulation platform will be to guide the design and optimization of closed-loop control for a specific case prior to its use. Validating this feature will bring Pulse Physiology Engine closer to a digital twin model of ECMO physiology.[6]

Declarations

Conflict of Interest Disclosure:

RU is a co-inventor on a patent application US20250205468A1 “Smart programmable blood pump for controlling and automating extracorporeal life support applications.” J.B.W., A.B., and R.C. are employees at Kitware, Inc.

Ethics Approval

Statement: For all animal studies, the Institutional Animal Care and Use Committee at Vanderbilt University Medical Center approved the protocol. The Animal Care and Use Review Office at the U.S.

Army Medical Research and Development Command also approved the protocol. The procedures were conducted according to the 'Principles of Laboratory Animal Care' by the National Society for Medical Research and the 'Guide for the Care and Use of Laboratory Animals' prepared by the Institute of Laboratory Animal Resources and published by the National Institutes of Health.

Patient consent statement

not applicable

Permission to reproduce material from other sources

One of the figures will be reused from a previous paper published by the corresponding author in *Scientific Reports*, and its reuse is permitted under a Creative Commons license.

Supporting Information

Supporting Information is available from the Wiley Online Library or from the author.

Funding:

This material is based upon work supported by the Defense Advanced Research Projects Agency (DARPA) under Contract No. N660012424024. The views, opinions, and/or findings expressed are those of the authors and should not be interpreted as representing the official views or policies of the Department of Defense or the U.S. Government. This work was also supported by grant 1S10OD038300-01 “Real-Time Blood Parameter Monitoring System” which was used to acquire Terumo CDI Blood Parameter Monitoring System 550. S.B. was funded by the NIH T32 Training Program for Innovative Engineering Research in Surgery and Intervention (T32EB021937).

Acknowledgements

We thank the S.R. Light Laboratory of the Vanderbilt Section of Surgical Sciences for their surgical support in obtaining the porcine VV-ECMO experiment data. We also appreciate Dr. Matthew Bacchetta’s input and feedback on the manuscript.

Data Availability Statement:

The programming scripts used to generate the *in silico* datasets in this study, as well as the animal data used for validations, will be made available on Kitware’s repository after the paper is accepted for publication.

Data Availability Statement

The programming scripts used to generate the *in silico* datasets in this study, as well as the animal data used for validations, will be made available on Kitware's repository after the paper is accepted for publication.

Received:

Revised:

Published online:

References

1. Extracorporeal Life Support Organization (ELSO) (2026)
2. Grant AA et al (2018) A Weaning Protocol for Venovenous Extracorporeal Membrane Oxygenation With a Review of the Literature. Artif Organs 42:605–610
3. Broman LM, Malfertheiner MV, Montisci A, Pappalardo F (2018) Weaning from veno-venous extracorporeal membrane oxygenation: how I do it. J Thorac Disease 10
4. Gannon WD et al (2021) Safety and Feasibility of a Protocolized Daily Assessment of Readiness for Liberation From Venovenous Extracorporeal Membrane Oxygenation. Chest 160:1693–1703
5. Zanella A et al (2016) A mathematical model of oxygenation during venovenous extracorporeal membrane oxygenation support. J Crit Care 36:178–186
6. Pladet L et al Clinical decision support for ExtraCorporeal Membrane Oxygenation: Will we fly by wire? - PubMed. Perfusion 38 (2023 May).
7. Joyce CJ et al (2018) A mathematical model of CO2, O2 and N2 exchange during venovenous extracorporeal membrane oxygenation. *Intensive Care Medicine Experimental* 6 (2018)
8. Ukita R et al (2026) Patient-specific, computational model of venovenous extracorporeal membrane oxygenation based on pulse physiology engine. Sci Rep
9. Schmidt M et al (2013) Blood oxygenation and decarboxylation determinants during venovenous ECMO for respiratory failure in adults. Intensive Care Med 39:838–846
10. Bray A et al (2019) Pulse Physiology Engine: an Open-Source Software Platform for Computational Modeling of Human Medical Simulation. SN Compr Clin Med 1:362–377
11. Webb JB et al (2020) Computational simulation to assess patient safety of uncompensated COVID-19 two-patient ventilator sharing using the Pulse Physiology Engine. PLoS ONE 15:e0242532
12. Glomp G et al (2026) Toronto, Canada,. in *Proceedings of the Annual International Conference of the IEEE Engineering in Medicine and Biology Society (EMBC)*
13. Bakdash JZ, Marusich LR (2019) Frontiers | Corrigendum: Repeated Measures Correlation. *Frontiers in Psychology* 10 /05/28)

14. Marusich LR, Bakdash JZ, Marusich LR, Bakdash JZ (2021) *rmcorrShiny: A web and standalone application for repeated measures correlation*. Vol. 10 /11/08)
15. Roberts KG, Nasim U, Hong Y, Cook KE, Ukita R (2026) Semi-Empirical Model to Predict Blood Flow in an Extracorporeal Respiratory Support Circuit Driven by Ventricular Assist Devices. *ASAIO Journal* online first
16. Takahashi K et al Simple and reliable method for predicting extracorporeal membrane oxygenation flow rates and circuit pressures. *Intensive Care Medicine Experimental 2026 14:1* 14 (2026-03-04)
17. Ganushchak Y, van Marken Lichtenbelt W, van der Nagel T, de Jong DS (2006) Hydrodynamic performance and heat generation by centrifugal pumps. Perfusion 21:373–379
18. Glomp G, Cortelli M, Bernicker B, Bacchetta M, Ukita R (2025) Open-access smart blood pump platform for controlling extracorporeal membrane oxygenation. HardwareX 22
19. Wang S et al (2019) Hemodynamic Evaluation of Avalon Elite Bi-Caval Dual Lumen Cannulas and Femoral Arterial Cannulas. Artif Organs 43:41–53
20. Sabetta G, Zhang X, Yang J, Zaidi S, Schwartz J (2026) Determinants of Baseline Membrane Lung Resistance in Extracorporeal Membrane Oxygenation. *Artif Organs*
21. Lehle K et al (2014) Flow Dynamics of Different Adult ECMO Systems: A Clinical Evaluation. Artif Organs 38:391–398
22. Abrams D, Bacchetta M, Brodie D (2015) Recirculation in Venovenous Extracorporeal Membrane Oxygenation. ASAIO J 61:115
23. Conrad SA, Wang D (2021) Evaluation of Recirculation During Venovenous Extracorporeal Membrane Oxygenation Using Computational Fluid Dynamics Incorporating Fluid-Structure Interaction. ASAIO J 67:943–953
24. Potter L et al (2017) /03/03 Physiology informed virtual surgical planning: a case study with a virtual airway surgical planner and BioGears. https://doi.org/10.1117/12.*2252510* 10135
25. Webb J, Bray A, Chimakurthi S, Clipp RA (2025) Heterogeneous Bronchopulmonary Computational Physiology Model for Multiphysics Analysis of Primary Blast Lung Injury
26. He G et al Flow characteristics and hemolytic performance of the new Breethe centrifugal blood pump in comparison with the CentriMag and Rotaflow pumps. Int J Artif Organs 44 (2021–2011)
27. Guan Y et al Evaluation of Quadrox-i® Adult Hollow Fiber Oxygenator with Integrated Arterial Filter. J Extracorpor Technol 42 (2010/06/01).
28. Tayama E et al (1997) Hemolysis Test of a Centrifugal Pump in a Pulsatile Mode: The Effect of Pulse Rate and RPM Variance. Artif Organs 21
29. Reagor J, Gao Z, Tweddell J (2021) Spectrum Medical Quantum or Terumo CDI 500: Which Device Measures Hemoglobin and Oxygen Saturation Most Accurately When Compared to a Benchtop Blood Analyzer? J Extracorpor Technol 53
30. Elgabori O et al (2026) Development of an Optical Sensor for Real-Time Monitoring of Hemodynamic Parameters in Extracorporeal Settings. IEEE J Translational Eng Health Med 14

31. Conway RG et al (2020) Evaluation of an autoregulatory ECMO system for total respiratory support in an acute ovine model. Artif Organs 44:478–487
32. Demarest CT et al (2020) The Time Course of Clinical Oxygenator Failure Due to Clot Formation

Figures

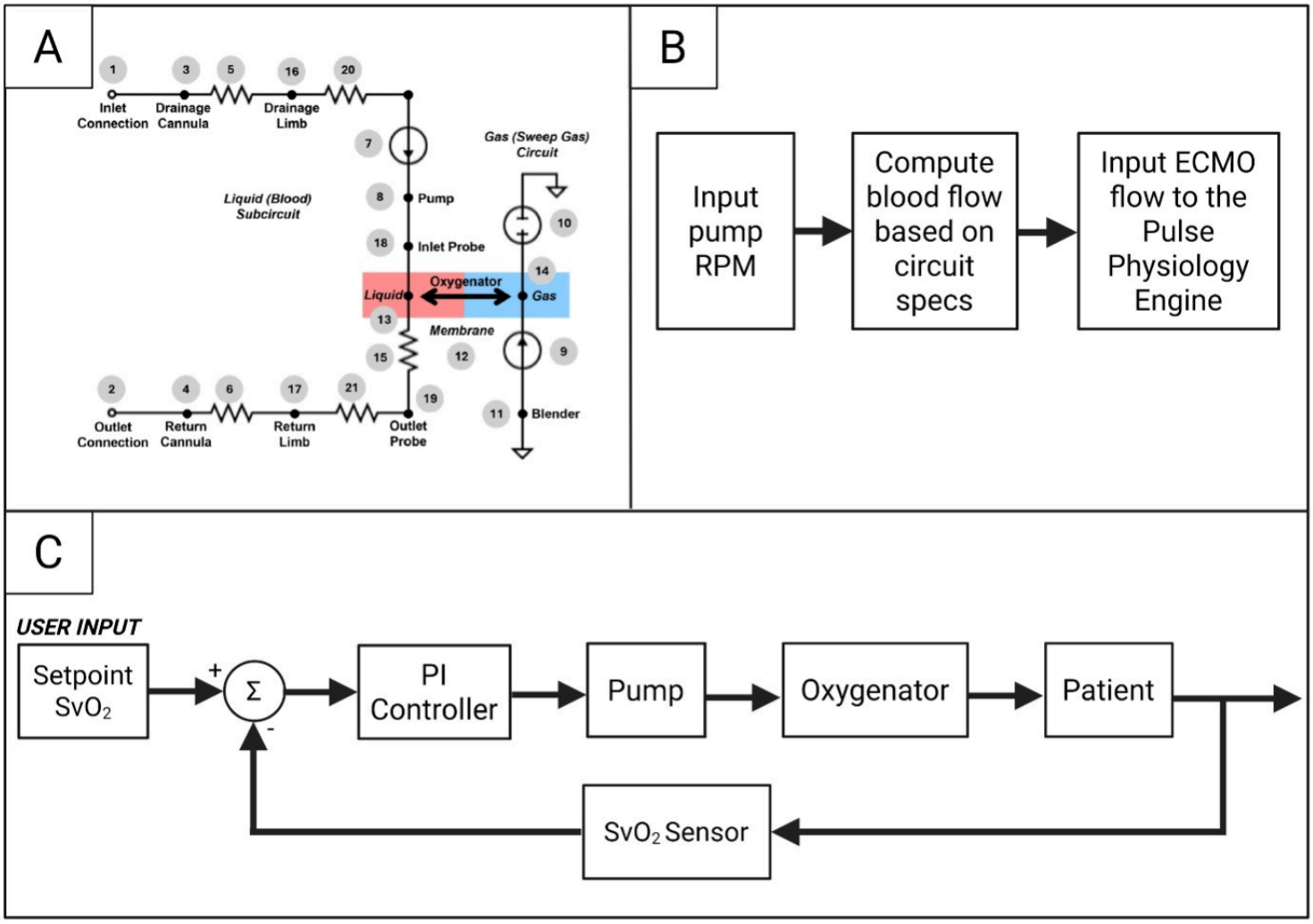


Figure 1

Schematic overview of the Pulse Physiology Engine platform for simulating venovenous extracorporeal membrane oxygenation (VV-ECMO): A) VV-ECMO circuit, B) block diagram relating pump speed input to corresponding blood flow rate, C) block diagram showing how proportional integral (PI) controller is implemented to maintain setpoint venous oxygen saturation (SvO_2). Panel A is reused from a previous publication,[8] permitted under a Creative Commons Attribution-NonCommercial-NoDerivatives 4.0 International License. The label for each number in panel A is provided in the supplements.

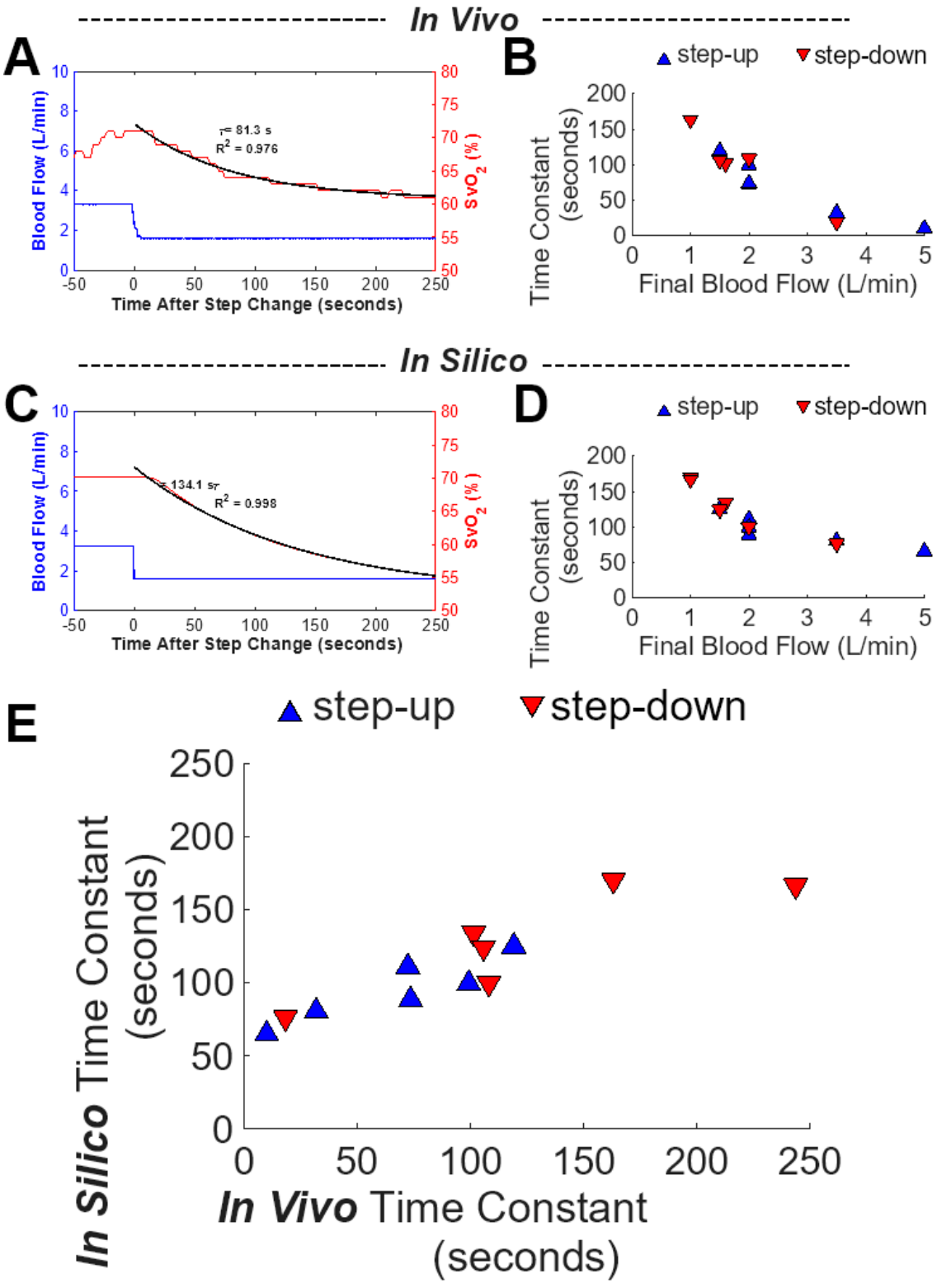


Figure 2

A) Transient venous oxyhemoglobin (SvO_2) kinetics were measured using Terumo inline sensor during in vivo porcine experiments (N=5) and also simulated in Pulse mirroring the animal study. B) SvO_2 time constants extracted from VV-ECMO experiments and C) Pulse simulations.

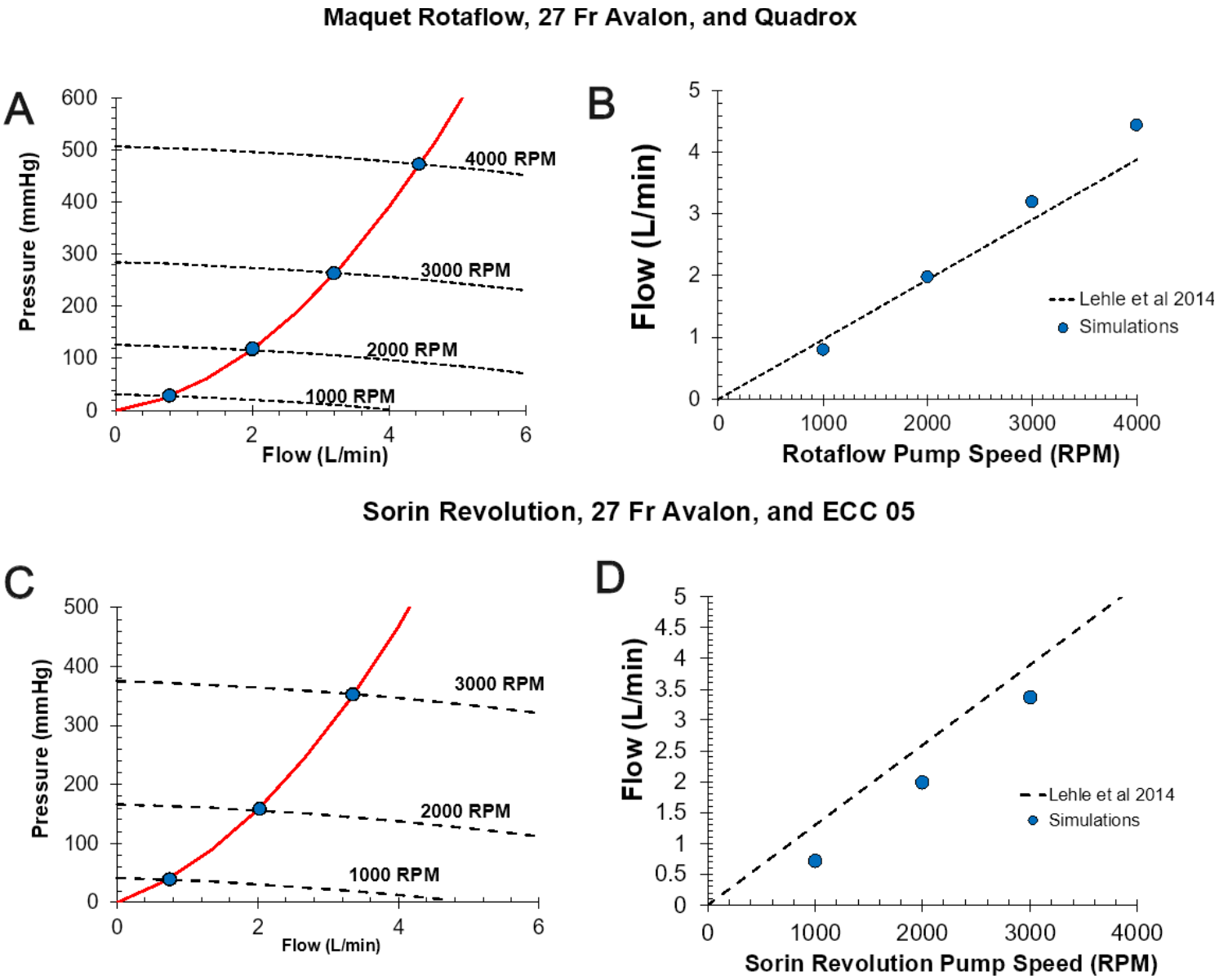


Figure 3

Blood flow rate calculations based on pump speed input and extracorporeal circuit characteristics: A) Maquet Rotaflow pump pressure-flow (HQ) curves plotted against the system curve from a 27-French dual-lumen Avalon cannula and a Quadrox oxygenator. Blue dots denote the intersection of the two sets of curves that represent the flow rate achieved for each pump speed in revolutions per minute (RPM). B) Predicted flow rate for the Maquet circuit at Rotaflow pump speed between 1000 and 4000 RPM. The dotted line represents clinical data taken from a 2014 study by Lehle et al. with the same set of pump, oxygenator, and cannula.[21] C) Sorin Revolution's HQ curves plotted against the system curve from a 27-French dual-lumen Avalon cannula and ECC05 oxygenator. D) Predicted flow rate for the Sorin circuit at speed between 1000 and 3000 RPM/ The dotted line again represents clinical data from the same Lehle et al study as panel B.

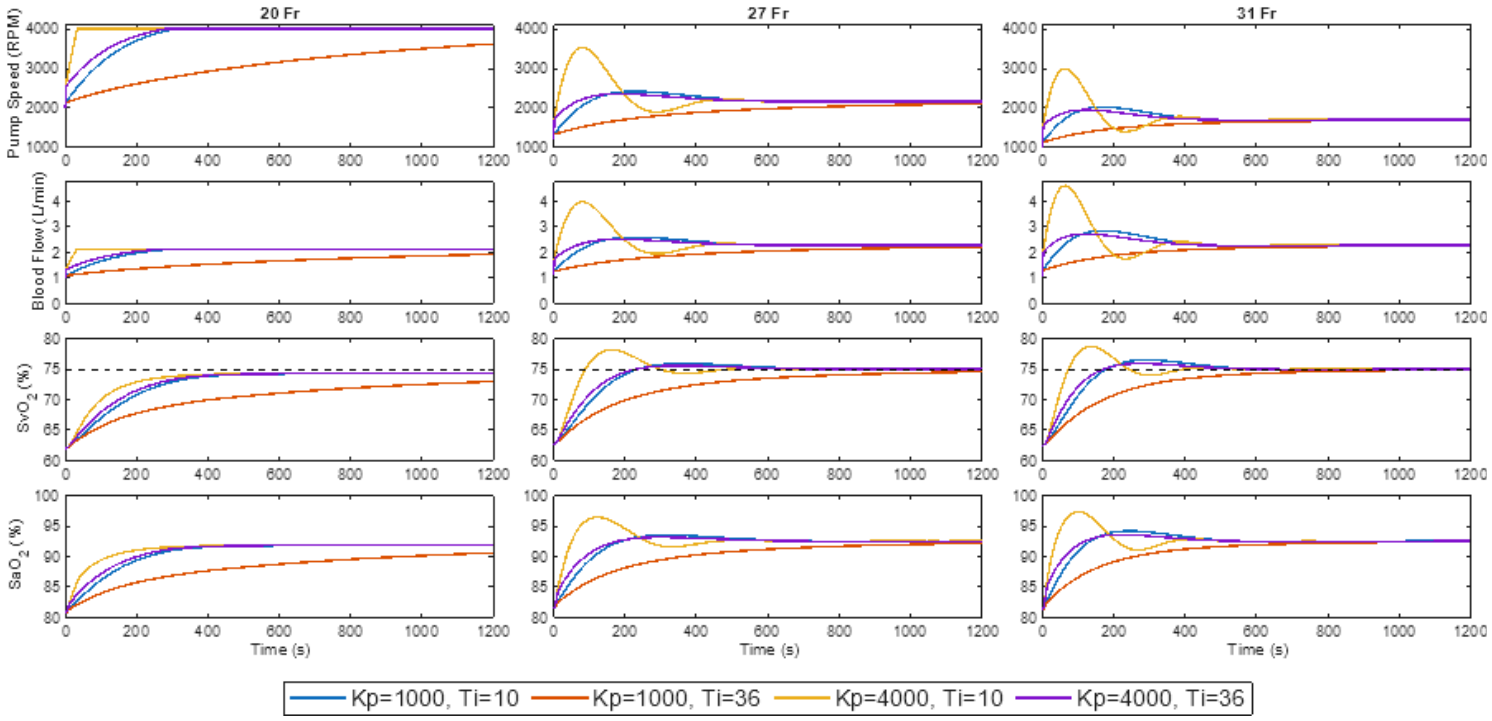


Figure 4

Closed-loop control of Maquet Rotaflow blood pump in a simulated male patient experiencing pulmonary shunt and being supported on venovenous extracorporeal membrane oxygenation. Proportional integral control strategy is used with four different combinations of gain settings for the proportional gain Kp and integral time Ti. Avalon cannula size is varied between 20 and 31 French. A) Pump speed and B) blood flow change in response to setpoint venous oxygen saturation (SvO2) of 75%. C) SvO2 and its setpoint shown as dotted line, D) and corresponding arterial saturation (SaO_2).

A

	FiO_2 (%)	Tidal Volume (mL)
baseline	100	200
	21	50
	50	100
	75	150

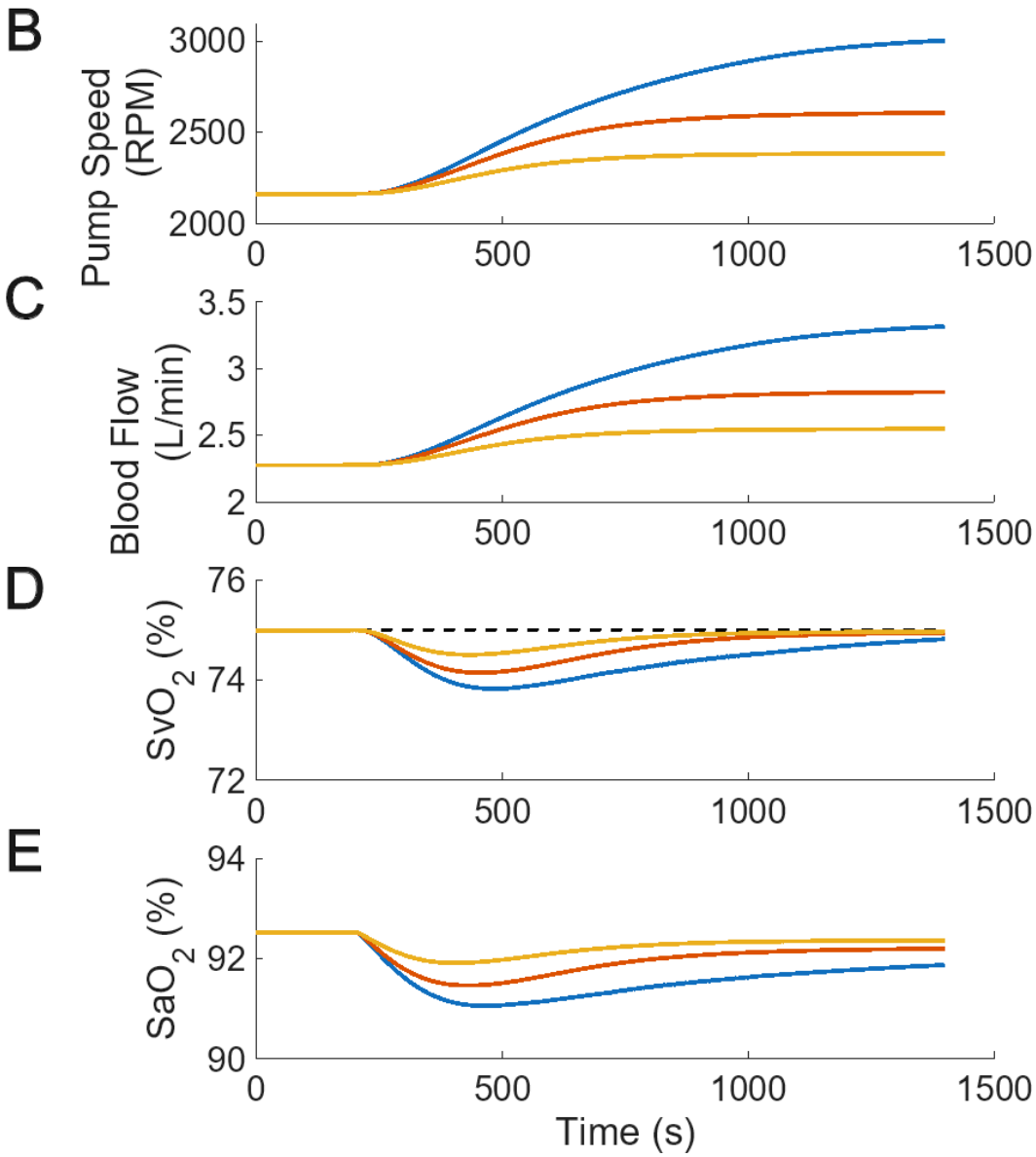


Figure 5

The closed-loop blood pump controller based on proportional integral control (Kp =4000, Ti = 10, setpoint SvO_2 = 75%) is evaluated using ventilator-induced respiratory disturbance scenarios. A) Table showing the baseline ventilator setting and the three different levels of disturbances caused by concomitant decrease in fraction of inspired oxygen (FiO_2) and tidal volume. Disturbance is induced at the 200-second mark. B) Pump speed C) blood flow rate, D) SvO_2, E) arterial saturation (SaO_2).

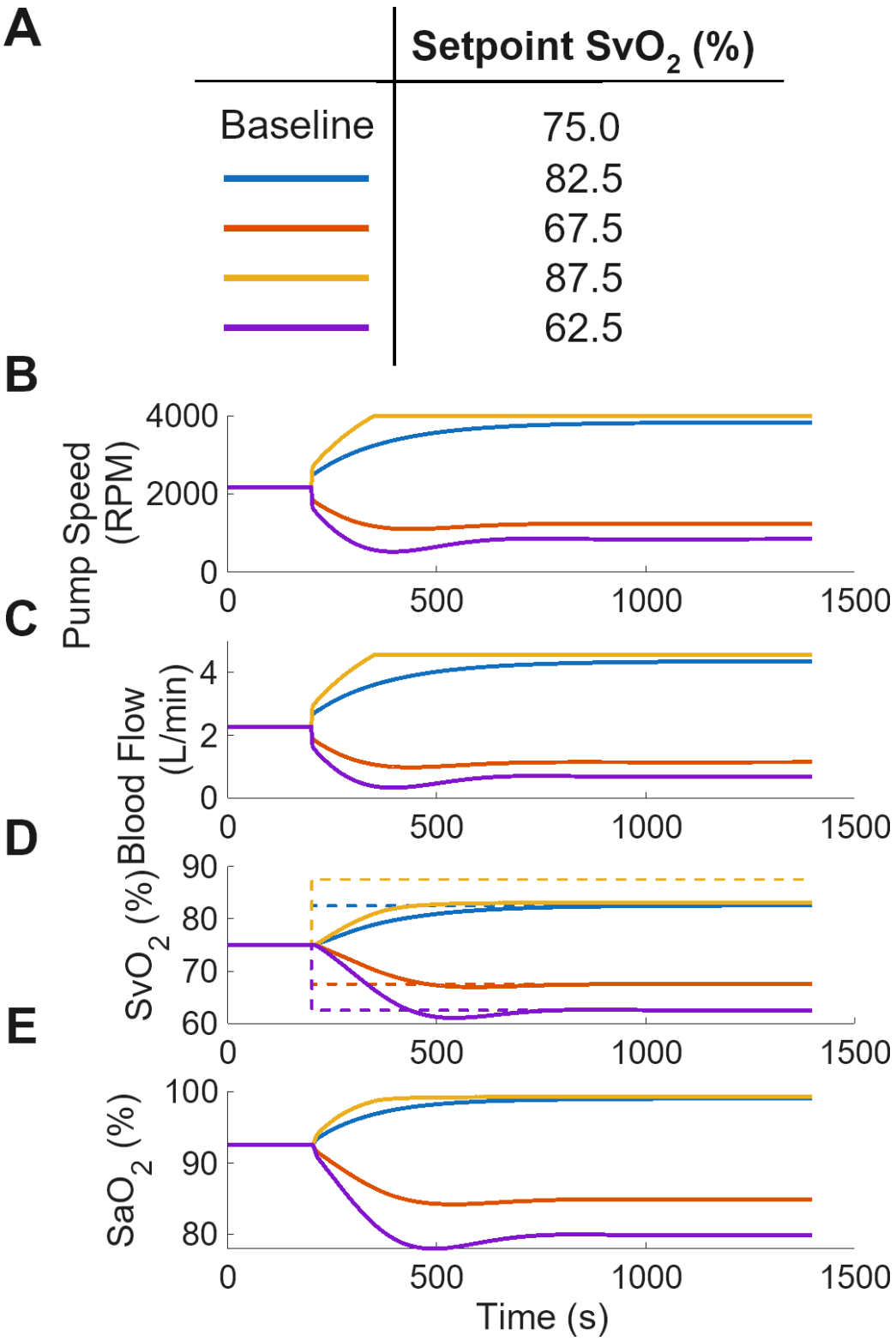


Figure 6

The closed-loop blood pump controller based on proportional integral control (Kp =4000, Ti = 10, initial setpoint SvO_2 = 75%) undergoing change in setpoint SvO_2. A) Table showing the starting setpoint and four different setpoints. Disturbance is induced at the 200-second mark. B) Pump speed C) blood flow rate, D) SvO_2, E) arterial saturation (SaO_2).

A

	stance (mmHg/(L/	O_2 Diffusion Capacity (mL/min/mmHg)
baseline	5.5	0.53
	11.0	0.30
	30.0	0.20
	55.0	0.10

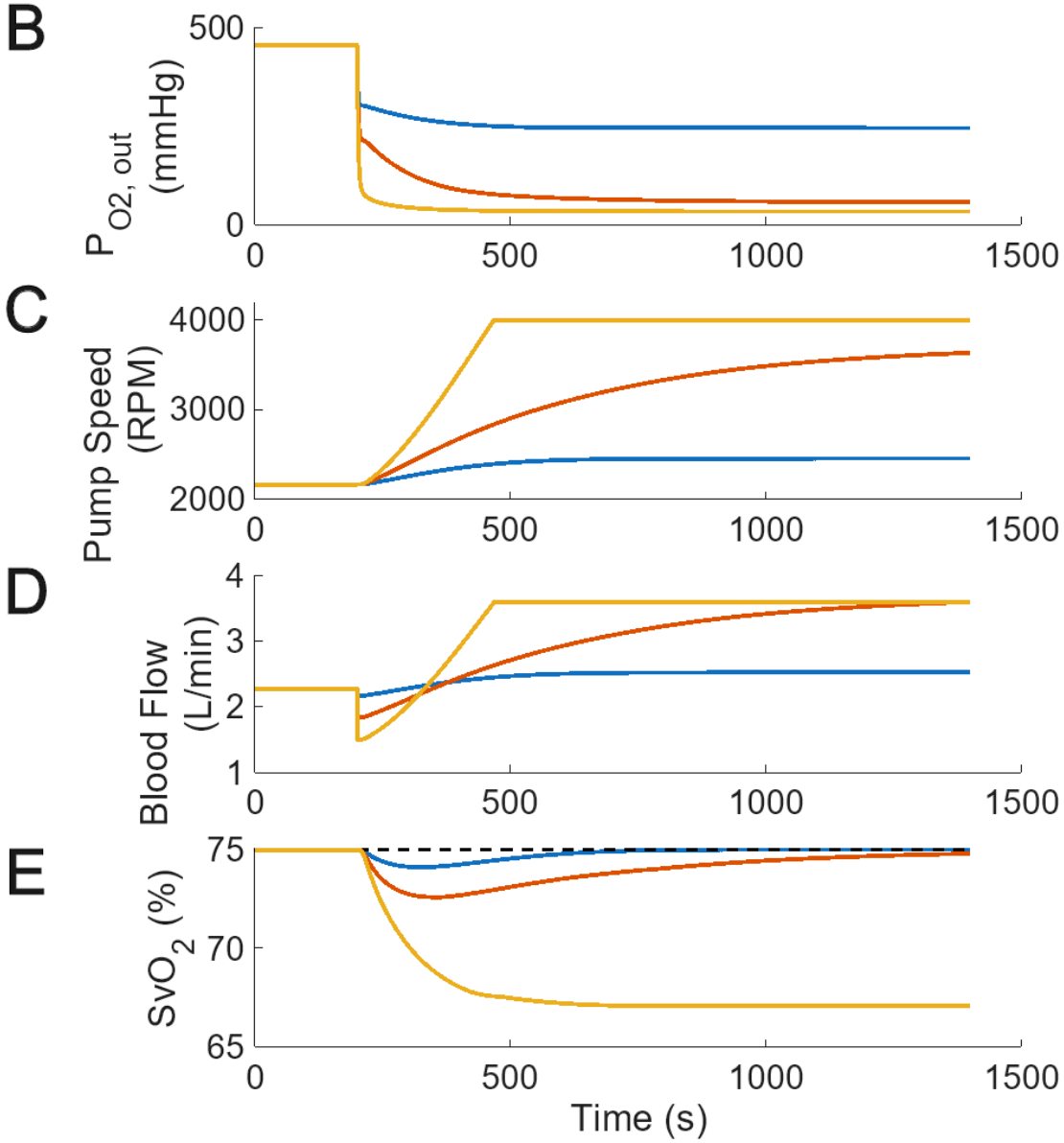


Figure 7

The closed-loop blood pump controller based on proportional integral control (Kp =4000, Ti = 10, setpoint SvO_2 = 75%) is evaluated against oxygenator thrombosis disturbance scenarios. A) Table showing the baseline levels of oxygenator resistance and oxygen diffusion capacity, and three different levels of thrombotic burden. Thrombosis disturbance is induced at the 200-second mark. B) Pump speed C) blood flow rate, D) SvO_2, E) arterial saturation (SaO_2).

Supplementary Files

This is a list of supplementary files associated with this preprint. Click to download.

- SupportingInformation.docx